

This Page Is Inserted by IFW Operations
and is not a part of the Official Record

BEST AVAILABLE IMAGES

Defective images within this document are accurate representations of the original documents submitted by the applicant.

Defects in the images may include (but are not limited to):

- BLACK BORDERS
- TEXT CUT OFF AT TOP, BOTTOM OR SIDES
- FADED TEXT
- ILLEGIBLE TEXT
- SKEWED/SLANTED IMAGES
- COLORED PHOTOS
- BLACK OR VERY BLACK AND WHITE DARK PHOTOS
- GRAY SCALE DOCUMENTS

IMAGES ARE BEST AVAILABLE COPY.

**As rescanning documents *will not* correct images,
please do not report the images to the
Image Problem Mailbox.**

REMARKS

The claims as filed were misnumbered beginning with claim 29 and the misnumbering is regretted. This has now been corrected.

Claims 1-3, 5, 7-10, 13-22, 25-30, 36, 37, 40, 42,43,46-53, 56-58, 62-64, 66, 68, 69, 72-79, 82, 83, 87-89, 91-94, 97-104, 106-108 and 112-117 are rejected under 35 U.S.C. 102(e) as being anticipated by U.S. Patent No. 5,963,329 to Conrad et al. ("Conrad"). Some of the rejected claims have been amended and the rejection is traversed in so far as it is applied tot he claims as amended. It is believed to be well established that for a reference to anticipate a claim, there must be identity of elements between the reference and the claim.

Conrad fails this test as applied to claim 1 as amended. Conrad fails to teach or suggest detecting changes in polarization state of the beam that is diffracted by the diffracting structure, providing a set of polarization state data and arriving at the values of one or more parameters of the diffracting structure from the measured changes in polarization state and from an optimized estimation within a neighborhood of the set of polarization state data that is provided. The Examiner points to column 4, lines 8-15, 28-56 and column 8 lines 1-15 of Conrad as showing the above features claimed in claim 1. None of the sections referred to by the Examiner disclose the features in claim 1. Column 4, lines 8-15 and 28-56 fail to teach anything even remotely resembling the above feature. In column 8, lines 1-15 Conrad describes a system for measuring parameters of a grating, where a polarizer 20 is used for providing polarized light column 4, lines 8-15, 28-56 directed to the grating for measurement. The use of polarized light for the measurement by Conrad permits the grating profile to be calculated independently

from two normal polarizations: transverse magnetic (TM) that transverse electric (TE). As noted by Conrad, the grating profile calculated from these two different polarizations give almost identical line profiles. Column 10, lines 35-55.

Since Conrad does not detect the polarization of light that is diffracted or reflected by the grating, it would be impossible for Conrad to detect the changes in polarization state caused by the diffraction/reflection. In contrast, such change in polarization state is measured in the invention of claim 1. As clearly described in the embodiment on page 9, lines 12-22 of the specification of the present application, an analyzer 32 is used to detect the polarization state of the radiation diffracted by the diffracting structure, and the change in polarization state of such radiation caused by the diffraction can be measured by rotating either the polarizer 28 or the analyzer 32 when spectrometer 34 is detecting the diffracted radiation passed by the analyzer and from the diffracting structure 60 at a plurality of wavelengths. The changes in polarization state data at different wavelengths can then be derived by computer 40 from the intensities detected by the spectrometer. While this embodiment is useful in illustrating the feature claimed in claim 1, the scope of claim 1 is not limited to such embodiment. The polarization state of radiation diffracted by the diffracting structure is also measured in this embodiment, which permits the detection of change in polarization state of radiation caused by the diffraction. This is in contrast to Conrad, which does not measure the polarization state of radiation diffracted by the diffracting structure. From the above, it is evident that Conrad does not measure change in polarization state of radiation caused by diffraction or reflection by the grating.

From the above, it is evident that there is no identity of elements between claim 1 and Conrad so that claim 1 is not anticipated by Conrad. As noted above, polarizer 20 is used by Conrad to enable two different independent calculations to be made, one in the TM mode and the other in TE mode, and not for the purpose for measuring the change in polarization state. There is therefore no reason or motivation to modify Conrad in order to measure change in polarization state caused by the diffraction/reflection by the diffracting structure. Claim 1 is therefore believed to allowable.

As for claim 21, the Examiner appears to have ignored the limitation that “the wavelengths of the intensity or change in polarization state data in the one or more sets are chosen as a function of the properties of the one or more layers,” where the diffracting structure measured is on or under such one or more layers when the measurement is carried out. This is not taught or suggested by Conrad. As explained in the embodiment of the invention on page 16, lines 11-23, polysilicon in the film stacks 16a and 16c over or below the diffracting structure is substantially opaque at wavelengths from the ultraviolet range to about 380 nm. Therefore, if the intensity or change in polarization state data that are analyzed are only those for this wavelength range, the effect of variations in optical characteristics of the top or bottom film stacks on the measurements can be essentially ignored. This will simplify the calculations. For example, if the profile of grating 16b is measured at wavelengths from the ultraviolet range to about 380 nm, the measurements will not change despite variations in the optical characteristics of the film stacks across the grating. While this one example illustrates the functionality of the feature claimed in claim 21, the scope of claim 21 is not limited to

such example. Conrad fails to teach or suggest such feature and claim 21 is therefore believed to be allowable.

The feature of claim 27 is illustrated by the embodiment of the description on page 17, lines 9-16. As clearly explained in such section and in Fig. 8, the diffraction intensity can change rapidly with a small change in wavelength at some wavelength values but changes rather slowly in other wavelength regions. To more accurately represent the shape of the curve, it is desirable to increase the density of the data samples within regions where the diffraction density changes rapidly with wavelength such as within regions 184 and 186. While such example illustrates the functionality of claim 27, the scope of claim 27 is not limited to such example. Conrad fails to teach or suggest any feature even remotely resembling such limitation. Claim 27 is therefore believed to be allowable.

Claims 2 and 3 are believed to be allowable since they depend from allowable claim 1, and further on the ground of the limitations in these claims. Claim 2 adds to claim 1 the generation of a library of sets of changes of polarizing state data and comparing measured changes in polarization state to the sets of data in the library, to define the set of change in polarization state data that corresponds to the first set of values of the one or more parameters. This is not taught or suggested by Conrad in the sections referred to by the Examiner or any other section.

Claim 5 is believed to be allowable since it depends from allowable claim 1. It is further believed to be allowable on the ground that it adds the limitation that the first set of values of the one or more parameters is chosen as a function of sensitivity of the change in polarization state data to changes in the one or more parameters. Column 5,

lines 28-47 referred to by the Examiner in the Office action does not teach or suggest such feature at all. Such section in Conrad merely describes a slab model for predicting a percentage of energy that is diffracted and has nothing to do with choosing the value of parameters as a function of the sensitivity of the change in polarization state data of the diffracted radiation.

Claims 7, 8, 25, 26, 29 and 30 are believed to be allowable since they depend from allowable claims.

The Examiner rejected claim 9 in view of column 9, lines 9-45 and column 4, lines 30-50 of Conrad. We respectfully disagree. While Conrad mentions the calculation of eigenvalues in column 9, line 37, Conrad fails to teach or suggest storing the eigenvalues and using the stored eigenvalues for obtaining the value of one or more parameters of the diffracting structure.

Models of the interaction between the beam of electromagnetic radiation and the grating are used for solving Maxwell's equations of such interaction. In the solution of the Maxwell's equations, the process decomposes the solution into a number of steps. An intermediate step in solving the equations is the derivation of the eigenvalues. The invention of claim 9 is based on the recognition that, for many diffracting structures, the initial steps for solving the Maxwell's equations are the same so that these steps do not need to be repeated every time but rather can be saved for future reference and reused, thereby saving time and effort in calculation. See for example the specification of the present application, page 13, line 21 through page 14, line 15. For this reason, the eigenvalues may be stored for future reference and can be reused to save time and calculation. This is not taught or suggested at all by Conrad.

From the above, it is clear that there is no identity of elements between claim 9 and Conrad. There is also no reason or motivation for modifying Conrad to arrive at the features of claim 9. Claim 9 is thus also nonobvious over Conrad and is therefore believed to be allowable.

Claim 10 is believed to be allowable since it depends from allowable claim 9 and because of the features of the claim. Claim 10 adds the limitation that the providing provides the model that accounts for the material(s) of the structure. This is not taught or suggested by Conrad. Column 5, lines 30-35 of Conrad referred to by the Examiner describes a slab model which does not take into account the type of material in the diffracting structure, unlike claim 10.

The Examiner rejected claims 13-18 in view of the disclosure in column 6, lines 6-30 of Conrad. We respectfully disagree. Column 6, lines 6-30 of Conrad describes the S profile used in models for predicting diffraction from the diffracting structure. The S profile is used as an approximation to the shape of the structure, and is thus radically different from and has nothing to do with the S-matrix in claims 13-18. The S-matrix is a mathematical representation that characterizes the reflection and transmission of radiation at an optical interface. For a more detailed explanation of the S-matrix please see the article enclosed by Lifeng Li, entitled "Formulation and comparison of two recursive matrix algorithms for modeling layered diffraction gratings," J. Opt. Soc. Am. A/Vol. 13, No. 5/May 1996.

Claims 19 and 20 are believed to be allowable since they depend from allowable claim 9.

Claim 22 is believed to be allowable since it depends from allowable claim 21. It is further believed to be allowable since it contains the limitation that the wavelengths of the intensity or change in polarization state data are chosen to reduce the influence of the properties of the one or more layers (above and/or below the diffracting structure) on deriving the value of the one or more parameters. When electromagnetic radiation is directed at the structure to perform measurements, the measurements will be affected by the effects of such layers on the measurements. Column 8, lines 15-35 referred to by the Examiner pertains to a process for normalizing the illumination intensity of the illumination source despite change in intensity of the source and has nothing to do with changing the wavelengths to reduce the influence of the properties of the film stacks on deriving the parameters. Claim 28 is believed to be allowable for substantially the same reasons as those above for claim 22.

For reasons similar to those described above for claims 1, 9, 21, and 27, claims 36, 42, 52 and 56 as amended are likewise believed to be allowable. These limitations are not taught in the sections of Conrad referred to by the Examiner (column 7, lines 60-column 8, line 14 and column 5, lines 38-50) or teachings in any other section of Conrad.

Claim 58 pertains to an apparatus for finding a value related to one more parameters of a 3-dimensional diffracting grating. Conrad has failed to teach or suggest such feature. It is noted, for example, that all of the models illustrated in the figures or described by Conrad are two-dimensional models which cannot be used by themselves for deriving parameters of a three-dimensional diffracting structure. Furthermore, two-dimensional models cannot be extended automatically in deriving parameters of three-dimensional diffracting structures. Since three-dimensional diffracting structures include

more variables and parameters that would need to be taken into account, and the number of variables that need to be taken into account in two-dimensional is already quite high, it is not obvious how the larger number of three-dimensional diffracting structures can also be taken into account to extend the two-dimensional models to three dimensions.

Based on the above, there is no identity of elements between claim 58 and Conrad and further that claim 58 is nonobvious over Conrad.

As for claims 37, 53 and 57, it is noted above that column 8, lines 15-35 teaches nothing more than normalizing the intensity of the illumination beam despite variations in the intensity of light from the illumination source, which has nothing to do with the features in these claims. These three claims are also believed to be allowable for such reason and since they depend from allowable claims.

Claim 40 is believed to be allowable since it depends from allowable claims and also on the grounds of limitations therein, that is, for the same reasons as those explained above for claims 5, 53 and 57. Column 5, lines 28-47 referred to by the Examiner fails to disclose any feature even remotely resembling that in claim 40.

For the same reasons as those explained above for claim 10, claim 43 is also believed to be allowable. Column 4, lines 35-40 of Conrad fails to disclose any feature resembling such feature in claim 43.

Claims 46-51 are believed to allowable for the same reasons as those discussed above for claims 13-18.

Claims 62-64, 66, 68, 69, 72-79, 81-83, 87-89, 91-94, 97-104, 106-108 and 112-117 are believed to be allowable for the same reasons as those discussed above for other rejected claims. As for claims 112-117, these are believed to be patentable over Conrad,

even in view of Conrad's disclosure in column 4, lines 20-27, since these two claims require that a processing instrument alters its one or more processing parameters in response to the set of value(s). Conrad's disclosure in column 4, lines 20-27 is nothing more than a very general statement that the values of the parameters such as line width obtained are "useful for monitoring or controlling a process." Nothing in such statement teaches or suggests that the values can be used for actually altering one or more processing parameters of the processing instrument such as a stepper or etcher. While not limited to the embodiment described in the specification of the present application, page 20, line 16 to page 21, line 7, this feature of claims 112 and 116 does permit an integrated single tool to be constructed, which measures a diffracting structure created using the processing instrument, and uses feedback control to correct any errors in the processing instrument.

Claims 4, 39, 65, and 90 are rejected under 35 U.S.C. 103(a) as being unpatentable over Conrad. The rejection is respectfully traversed.

These four claims are believed to be allowable since they depend from allowable claims. They are further believed to be allowable since they add the limitation of performing non-linear regression which is not taught or suggested by Conrad. The examiner admits that Conrad fails to disclose such feature, but has failed to cite any factual support for concluding that this limitation would have been obvious in view of Conrad. The reason used in the rejection, namely that "this amounts to the use of a different or preferred method of data analysis," assuming arguendo to be true, still does not lead to the conclusion that this limitation, admitted by the examiner to be absent from Conrad, would have been obvious in view of Conrad.


We appreciate the Examiner's indication that claims 6, 11, 12, 23, 24, 38, 41, 44, 45, 54, 55, 67, 70, 71, 80, 81, 95, 96, 98 and 105 would be allowable if rewritten in independent form. This has not been done since the claims upon which they depend are also believed to be allowable.

Claims 118-139 have been added to more completely claim the invention; these claims are likewise believed to be patentable over Conrad and all other art of record.

Claims 1-30, 36-58, 62-83, 87-108 and 112-139 are presently pending in the application. Reconsideration of the rejections is respectfully requested and an early indication of the allowability of all of the claims is earnestly solicited.

<p align="center"><u>Certificate of Mailing Under 37 CFR 1.8</u></p> <p>I hereby certify that this correspondence is being deposited with the United States Postal Service with sufficient postage as first class mail in an envelope address to: Commissioner for Patents, P.O. Box 1450, Alexandria, VA 22313-1450, on <u>3/15/04</u></p> <p><u>Franklin</u> Signature</p>
--

Respectfully submitted,


James S. Hsue
Reg. No.: 29,545

Formulation and comparison of two recursive matrix algorithms for modeling layered diffraction gratings

Lifeng Li

Optical Sciences Center, University of Arizona, Tucson, Arizona 85721

Received July 20, 1995; revised manuscript received November 13, 1995; accepted December 4, 1995

Two recursive and numerically stable matrix algorithms for modeling layered diffraction gratings, the *S*-matrix algorithm and the *R*-matrix algorithm, are systematically presented in a form that is independent of the underlying grating models, geometries, and mountings. Many implementation variants of the algorithms are also presented. Their physical interpretations are given, and their numerical stabilities and efficiencies are discussed in detail. The single most important criterion for achieving unconditional numerical stability with both algorithms is to avoid the exponentially growing functions in every step of the matrix recursion. From the viewpoint of numerical efficiency, the *S*-matrix algorithm is generally preferred to the *R*-matrix algorithm, but exceptional cases are noted. © 1996 Optical Society of America

1. INTRODUCTION

As research in the field of diffraction gratings advances and the range of grating applications widens, the structures of gratings become more complicated than before. One of many new types of gratings that are finding more applications is layered gratings. For example, multi-layer thin films were deposited onto photoresist surface-relief gratings to make high-efficiency, all-dielectric reflection gratings,¹ and coating polycarbonate lamellar gratings with a layer of MgF_2 was proposed as a means of making broadband antireflection structures.² Perhaps the most extreme cases of layered gratings are the Bragg-Fresnel gratings for use in x-ray spectroscopy³ and the photonic band-gap materials.⁴ On the other hand, in some grating models even a grating that consists of a single periodically corrugated surface is treated numerically as a layered structure. In this paper the term layered gratings will be used broadly to refer to both physically and numerically layered periodic structures.

All numerical methods for analyzing layered gratings face a common difficulty associated with the exponential functions of the spatial variable in the direction perpendicular to the grating plane. This difficulty is indicative of many problems of wave propagation and scattering in layered systems, and it is exacerbated by the fact that accurate numerical analysis of gratings usually requires a large number of eigenmodes. Recently this numerical difficulty has been overcome by many authors.⁴⁻¹⁵ First, Pai and Awada⁵ presented a Bremmer series method, based on the modal analysis with Fourier expansions, for dielectric gratings of arbitrary profile and groove depth in TE polarization. At the same time, DeSandre and Elson⁶ presented an extinction-theorem analysis of diffraction anomalies in multilayer-coated shallow gratings by using the *R*-matrix propagation algorithm. Later, Li⁷ applied the *R*-matrix algorithm to the classical modal method and enabled the latter to treat gratings

of arbitrary profile, depth, and permittivity. Chateau and Hugonin⁸ proposed an algorithm, with the coupled-wave method, to model surface relief and volume gratings made of lossless and lossy dielectric materials. Montiel and Nevère⁹ applied the *R*-matrix algorithm to the differential method and thereby eliminated "the numerical instabilities that have plagued the differential theory in TM polarization during the past 20 years (Ref. 9, p. 3241). Recently Li¹⁰ applied the *R*-matrix algorithm to the differential formalism of Chandezon *et al.* (the C method) and thus removed a formerly existing limitation of the C method. The same goal was later achieved by Cotter *et al.*¹¹ using a scattering-matrix approach (*S*-matrix algorithm). The *S*-matrix algorithm was also used by Maystre⁴ in an electromagnetic study of photonic band gaps by the integral method. Additionally, Li¹² showed that under certain conditions the *S*-matrix algorithm (which, unfortunately, was referred to there as the *R*-matrix algorithm) and the Bremmer series algorithm are equivalent. Very recently, Moharam *et al.*¹³ presented another stable algorithm, which they call the enhanced transmission matrix approach. For references concerning the applications of the *S*-matrix and *R*-matrix algorithms to problems of wave propagation and scattering outside the field of diffraction gratings, the reader may consult the reference list in Ref. 12.

Now there exist many stable numerical algorithms and several variants of implementation, expressed with different terminologies and applied to different grating models. There are obvious similarities and subtle differences among these algorithms and their variants. Their advantages and disadvantages, as well as interrelationships, have not been addressed in the literature. The purpose of this paper is to provide a systematic and unified presentation of the *S*-matrix and *R*-matrix algorithms, independent of the underlying grating models (integral, differential, modal, etc.) being used and the incidence conditions (TE, TM, or conical mount), and to

compare these two algorithms in terms of their physical interpretations, numerical stabilities, and numerical efficiencies. Some results presented here have already appeared in the literature, but many intricate details are new.

The algorithmic structure of the S -matrix and R -matrix algorithms is recursive, and the matrix dimension in the recursion is independent of the number of layers. Meanwhile, there exist stable and nonrecursive algorithms, for example, those in Refs. 14 and 15. In these algorithms the field amplitudes in all layers are solved together from a large linear system of equations whose matrix dimension is proportional to the number of the layers. The nonrecursive algorithms and the recursive algorithm of Moharam *et al.*,¹² which has a structure different from that of the S -matrix and R -matrix algorithms, are not considered in this paper.

In what follows, first the framework is laid down, in Section 2, for the development in the subsequent sections by defining the notation and the basis functions. The S -matrix algorithm and the R -matrix algorithm are presented in Sections 3 and 4, respectively. The presentations are arranged as parallel as possible for the two algorithms to bring out their similarities. Several variants of the two algorithms are then given in Section 5. In Section 6 the two algorithms are compared in terms of their numerical stabilities and efficiencies. Finally, in Section 7 some remarks are made that are specific to the applications of the algorithms to several grating models.

2. BACKGROUND FRAMEWORK

A. Layer Abstraction

Figure 1 depicts a multilayer surface-relief grating. We assume that the profiles of all medium interfaces have the same periodicity in the x direction and that they are invariant in the z direction. We say that two adjacent interfaces are separable if a line $y = \text{constant}$ can be drawn between them without crossing either interface; otherwise, we say that they are nonseparable. Thus the bottom three interfaces in Fig. 1 are separable, and the top three are not.

The S -matrix and R -matrix algorithms are applicable to all grating models, but here the discussion will be restricted to the classical modal method, the C method, the coupled-wave method, and the differential method. When it is not necessary to make the distinction, the first three methods will be referred to collectively as the modal methods, because they all rely on finding eigenmodes of Maxwell's equations. The classical modal method and the coupled-wave method approximate a continuous profile by a stack of lamellar gratings, as illustrated in the triangular grating in Fig. 1. This numerical approximation effectively introduces a number of numerical layer interfaces. The differential method does not use the multilayer lamellar grating approximation, but for numerical purposes it decomposes a grating profile into thin horizontal slices, thus also creating numerical layer interfaces. If two adjacent medium interfaces have identical functional form and amplitude, the C method does not require any numerical layer interface; otherwise, one numerical interface may be needed between the two medium interfaces.^{16,17}

We abstract a layered grating structure by a series of parallel straight lines, each representing a real or numerical, straight or curved interface, depending on the profile of the medium interface and the grating model being used [see Fig. 2(a)]. For example, suppose that for the layered grating shown in Fig. 1 we use the classical modal method to treat the rectangular profile, the same method with a three-layer approximation to treat the triangular profile, the differential method with a three-slice decomposition to treat the asymmetrical smooth profile, and the C method to treat the top three profiles. Then, in Fig. 2(a), $n = 15$, 2 for the rectangular profile, 4 for the triangular profile, 4 for the asymmetrical smooth profile, and 6 for the top three profiles. The permittivities in Fig. 2(a) may be either constants or periodic functions of x , depending on the spatial region and the grating model. Media 0 and $n + 1$ are two semi-infinite homogeneous media. The dashed line in medium 0 is a numerical interface. It can be ar-

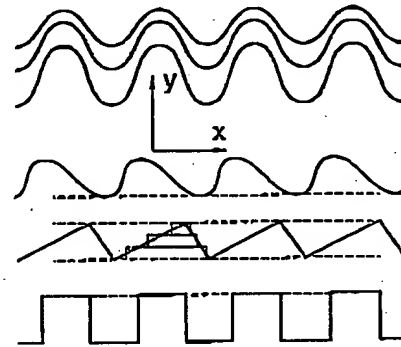


Fig. 1. General layered grating. All periodic medium interfaces share a common period, but otherwise they are arbitrary.

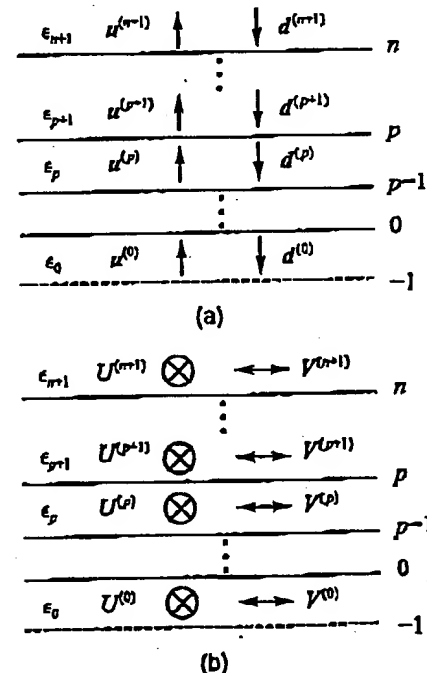


Fig. 2. Abstract layered grating structure, where the horizontal lines represent either actual material interfaces or numerical interfaces. The fields in each layer can be represented either (a) as a superposition of upward- and downward-propagating and decaying waves or (b) as a superposition of two sets of orthogonally polarized eigenmodes.

ararily close to interface 0. The thickness of layer p will be denoted by h_p .

1. Basis Functions

When a modal method is used to analyze layer p in Fig. 2(a), the fields there are represented by superpositions of the eigenmodes. We assume that the eigenmodes in all layers share a common Floquet exponent, which is determined by the incident plane wave. The eigenvalue spectrum $\sigma^{(p)}$, having elements $\lambda_m^{(p)}$, can be partitioned such that $\sigma^{(p)} = \sigma^{(p)+} \cup \sigma^{(p)-}$, where

$$\sigma^{(p)} = \{\lambda_m^{(p)}; \operatorname{Re} \lambda_m^{(p)} + \operatorname{Im} \lambda_m^{(p)} \geq 0, \lambda_m^{(p)} \in \sigma^{(p)}\}. \quad (1)$$

In general, for any numerical truncation, $\sigma^{(p)+}$ and $\sigma^{(p)-}$ have the same number of elements. The dependence of the eigenmodes on y , i.e., the y -dependent basis functions, is given by $\exp[i\lambda_m^{(p)} y]$, where $\lambda_m^{(p)} \in \sigma^{(p)}$. (Here y should be replaced by u if the C method is used; however, for simplicity we will ignore this minor difference.) Thus we call an eigenmode corresponding to $\lambda_m^{(p)+}$ an up wave, and that corresponding to $\lambda_m^{(p)-}$ a down wave. In particular, in the two semi-infinite regions and the homogeneous regions between the separable medium interfaces, the eigenmodes are simply the Rayleigh modes. In Fig. 2(a) the upward and downward arrows schematically represent the up wave and down waves, and the boldface letters u and d denote the column vectors whose elements are the wave amplitudes. Once the eigenmodes are determined everywhere, the grating problem reduces to a problem of determining the mode amplitudes.

Alternatively, we can choose $\cos(\lambda_m^{(p)+} y)$ and $\sin(\lambda_m^{(p)+} y)$ as the basis functions, which is always possible because $\lambda_m^{(p)-} = -\lambda_m^{(p)+}$ with the classical modal method and the coupled-wave method and with the C method when the grating profile is symmetrical. We use U and V to denote the amplitudes of the modes that use this basis function set. The physical meaning of these amplitudes is clear: for example, if U is proportional to the z component of the electric field, then V is proportional to the x components of the magnetic field, as schematically shown in Fig. 2(b). From a mathematical point of view, the derivative of a U mode is a V mode, and vice versa. For the modal methods, both the exponential (or u - d) basis functions and the trigonometrical (or U - V) basis functions can be used.

In the differential method, one does not seek the eigen-solutions of Maxwell's equations. Instead, one numerically integrates U from one interface to another, where U is a column vector whose elements are the Fourier expansion coefficients of the z component of the electromagnetic fields. The numerical integration procedure gives the values of U and $V = dU/dy$ as functions of y . Clearly, the U - V basis functions described here correspond to the U - V basis functions described in the preceding paragraph. Thus the schematic diagram in Fig. 2(b) applies to the differential method as well. It is possible to have a set of u - d basis functions for the differential method if suitable linear combinations are made.⁹ It is important to realize that, although the basis functions for the differential method do not have an explicit y dependence, their y dependence is asymptotically the same as that of the basis functions in the modal methods.

C. Boundary Conditions

In this subsection we affix the equation numbers of all equations that apply only to the u - d basis functions with a letter a , and those that apply only to the U - V basis functions with a letter b . The same convention will be used for the formulas of the S -matrix and R -matrix algorithms in Sections 3, 4, and 5.

In the modal methods, when the boundary conditions are matched along interface p , we generally get an equation of form

$$W^{(p+1)} \begin{bmatrix} u^{(p+1)}(y_p + 0) \\ d^{(p+1)}(y_p + 0) \end{bmatrix} = W^{(p)} \begin{bmatrix} u^{(p)}(y_p - 0) \\ d^{(p)}(y_p - 0) \end{bmatrix}, \quad (2a)$$

where $W^{(p)}$ and $W^{(p+1)}$ are square matrices. Furthermore, by virtue of the modal fields,

$$\begin{bmatrix} u^{(p)}(y_p - 0) \\ d^{(p)}(y_p - 0) \end{bmatrix} = \phi^{(p)} \begin{bmatrix} u^{(p)}(y_{p-1} + 0) \\ d^{(p)}(y_{p-1} + 0) \end{bmatrix}, \quad (3a)$$

where

$$\phi^{(p)} = \begin{bmatrix} \exp(i\lambda_m^{(p)+} h_p) & 0 \\ 0 & \exp(i\lambda_m^{(p)-} h_p) \end{bmatrix}, \quad (4a)$$

and the exponential functions represent diagonal matrices (henceforth, all quantities with a subscript m represent diagonal matrices). Thus we obtain a recursive relation for the field amplitudes

$$\begin{bmatrix} u^{(p+1)}(y_p + 0) \\ d^{(p+1)}(y_p + 0) \end{bmatrix} = \tilde{T}^{(p)} \begin{bmatrix} u^{(p)}(y_{p-1} + 0) \\ d^{(p)}(y_{p-1} + 0) \end{bmatrix}, \quad (5a)$$

where

$$\tilde{T}^{(p)} = \epsilon^{(p)} \phi^{(p)}, \quad (6)$$

with

$$\epsilon^{(p)} = W^{(p+1)-1} W^{(p)}. \quad (7)$$

The matrices $\epsilon^{(p)}$ and $\tilde{T}^{(p)}$ can be fittingly called interface and layer t matrices, respectively. Note that $\epsilon^{(p)}$ is of order $O(1)$.¹⁸

If the U - V basis functions are used to match the boundary conditions, we have, correspondingly,

$$W^{(p+1)} \begin{bmatrix} U^{(p+1)}(y_p + 0) \\ V^{(p+1)}(y_p + 0) \end{bmatrix} = W^{(p)} \begin{bmatrix} U^{(p)}(y_p - 0) \\ V^{(p)}(y_p - 0) \end{bmatrix}, \quad (2b)$$

$$\begin{bmatrix} U^{(p)}(y_p - 0) \\ V^{(p)}(y_p - 0) \end{bmatrix} = \phi^{(p)} \begin{bmatrix} U^{(p)}(y_{p-1} + 0) \\ V^{(p)}(y_{p-1} + 0) \end{bmatrix}, \quad (3b)$$

$$\phi^{(p)} =$$

$$\begin{bmatrix} \cos(\lambda_m^{(p)} h_p) & \eta_m^{(p)} \sin(\lambda_m^{(p)} h_p) \\ -\eta_m^{(p)-1} \sin(\lambda_m^{(p)} h_p) & \cos(\lambda_m^{(p)} h_p) \end{bmatrix}, \quad (4b)$$

$$\begin{bmatrix} U^{(p+1)}(y_p + 0) \\ V^{(p+1)}(y_p + 0) \end{bmatrix} = \tilde{T}^{(p)} \begin{bmatrix} U^{(p)}(y_{p-1} + 0) \\ V^{(p)}(y_{p-1} + 0) \end{bmatrix}. \quad (5b)$$

In Eq. (4b), $\eta_m^{(p)}$ is a constant independent of h_p , and for simplicity the plus sign has been dropped from the superscript of eigenvalue $\lambda_m^{(p)+}$. Also, the same notation

W , ϕ , and ϵ is used with the two different basis function sets. This, however, is not a problem because the context will tell to which basis the matrices are referring. From now on, the amplitude vectors without an explicit argument stand for the vectors that are evaluated at the lower bound of the layer. For example, $u^{(p)} = u^{(p)}(y_{p-1} + 0)$.

At this point, it is most natural and mathematically simplest to proceed with solving the grating problem by the so-called T -matrix algorithm, which is obtained by repeated use of Eq. (5a) or Eq. (5b). However, it is well known that the T -matrix algorithm, with either of the basis function sets, is numerically unstable when the total layer thickness of the grating structure and the matrix dimension are large.⁷ This numerical instability is generally attributed to the presence of the growing exponential functions in the algorithm. Fundamentally, the cause of instability is a classic one: loss of significant digits when one is computing a small number by subtracting two large numbers by a computer of finite precision. Symbolically, it is a case of $\infty - \infty = O(1)$. It should be emphasized that the numerical instability of the T -matrix algorithm cannot be eased or removed by simply reducing the individual layer thicknesses without lowering the total thickness, because the T -matrix algorithm accumulates the magnitudes of the exponential functions as the layer t matrices are multiplied together.

3. S-MATRIX ALGORITHM

The S -matrix algorithm uses the exponential basis functions. For any $0 \leq p \leq n$, it seeks a stack S matrix, $S^{(p)}$, that links the waves in layer $p + 1$ and medium 0 in this way:

$$\begin{bmatrix} u^{(p+1)} \\ d^{(0)} \end{bmatrix} = S^{(p)} \begin{bmatrix} u^{(0)} \\ d^{(p+1)} \end{bmatrix}. \quad (8a)$$

Before moving on, it is important to describe the physical meaning of the S matrix. For this purpose we rewrite $S^{(p)}$ in a two-by-two block form:

$$\begin{bmatrix} u^{(p+1)} \\ d^{(0)} \end{bmatrix} = \begin{bmatrix} T_{uu}^{(p)} & R_{ud}^{(p)} \\ R_{du}^{(p)} & T_{dd}^{(p)} \end{bmatrix} \begin{bmatrix} u^{(0)} \\ d^{(p+1)} \end{bmatrix}. \quad (9a)$$

The significance of the subscripts u and d becomes evident once the reader mentally carries out the matrix-vector multiplication on the right-hand side of the equation. As a rule in this paper, the use of subscripts u and d is an automatic indication that the submatrix belongs to a matrix in the S -matrix algorithm. The choice of letters R and T , instead of S , makes the physical meanings of the four submatrices of $S^{(p)}$ self-explanatory. For example, $T_{uu}^{(p)}$ and $R_{ud}^{(p)}$ are the transmission matrix and reflection matrix that give the upward wave amplitudes in layer $p + 1$ resulting from the transmission of the upward incident waves in medium 0 and from the reflection of the incident downward waves in layer $p + 1$, respectively, by the whole stack below layer $p + 1$. Alternatively, the first p layers of the layered grating can be viewed as a linear four-terminal network. Matrix $S^{(p)}$ operates on the two sets of inputs to generate the two sets of outputs, as shown schematically in Fig. 3(a).

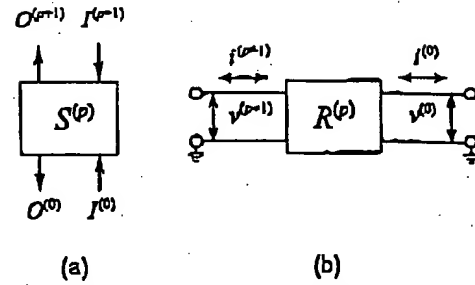


Fig. 3. Schematic diagrams for alternative interpretations of (a) the S matrix and (b) the R matrix. In Fig. 3(a), I and O stand for inputs to and outputs from the system represented by the square box. In Fig. 3(b), i and v stand for currents and voltages at the terminals of the circuit represented by the square box.

To link the waves in two adjacent layers, we can define an interface s matrix, $s^{(p)}$, and a layer s matrix, $\bar{s}^{(p)}$, as follows:

$$\begin{bmatrix} u^{(p+1)}(y_p + 0) \\ d^{(p)}(y_p - 0) \end{bmatrix} = s^{(p)} \begin{bmatrix} u^{(p)}(y_p - 0) \\ d^{(p+1)}(y_p + 0) \end{bmatrix}, \quad (10a)$$

$$\begin{bmatrix} u^{(p+1)} \\ d^{(p)} \end{bmatrix} = \bar{s}^{(p)} \begin{bmatrix} u^{(p)} \\ d^{(p+1)} \end{bmatrix}, \quad (11a)$$

or

$$\begin{bmatrix} u^{(p+1)} \\ d^{(p)} \end{bmatrix} = \begin{bmatrix} t_{11}^{(p)} & \bar{r}_{ud}^{(p)} \\ \bar{r}_{du}^{(p)} & t_{22}^{(p)} \end{bmatrix} \begin{bmatrix} u^{(p)} \\ d^{(p+1)} \end{bmatrix}. \quad (12a)$$

The physical interpretations of $s^{(p)}$ and $\bar{s}^{(p)}$ are similar to that of $S^{(p)}$. Note that $\bar{r}_{ud}^{(p)}$ and $\bar{r}_{du}^{(p)}$, because of the notation of their subscripts, cannot be confused with the t matrix defined in Section 2. The layer s matrix is related to the interface s matrix by

$$\bar{s}^{(p)} = \begin{bmatrix} 1 & 0 \\ 0 & \exp(-i\lambda_m^{(p)} h_p) \end{bmatrix} s^{(p)} \begin{bmatrix} \exp(i\lambda_m^{(p)} h_p) & 0 \\ 0 & 1 \end{bmatrix}, \quad (13a)$$

and the interface s matrix is in turn related to the interface t matrix by

$$s^{(p)} = \begin{bmatrix} t_{11}^{(p)} - t_{12}^{(p)} t_{22}^{(p)-1} t_{21}^{(p)} & t_{12}^{(p)} t_{22}^{(p)-1} \\ -t_{22}^{(p)-1} t_{21}^{(p)} & t_{22}^{(p)-1} \end{bmatrix}. \quad (14a)$$

Note that all four entries in Eq. (14a) contain the inverse of submatrix $t_{22}^{(p)}$. For this reason we call $t_{22}^{(p)}$ the pivotal submatrix.

From Eqs. (8a) and (11a), the set of recursion formulas for the stack S matrix are

$$\begin{aligned} T_{uu}^{(p)} &= \bar{t}_{uu}^{(p)} [1 - R_{ud}^{(p-1)} \bar{r}_{du}^{(p-1)}]^{-1} T_{uu}^{(p-1)}, \\ R_{ud}^{(p)} &= \bar{r}_{ud}^{(p)} + \bar{t}_{uu}^{(p)} R_{ud}^{(p-1)} [1 - \bar{r}_{du}^{(p-1)} R_{ud}^{(p-1)}]^{-1} \bar{t}_{dd}^{(p)}, \\ R_{du}^{(p)} &= R_{du}^{(p-1)} + T_{dd}^{(p-1)} \bar{r}_{du}^{(p-1)} [1 - R_{ud}^{(p-1)} \bar{r}_{du}^{(p-1)}]^{-1} T_{uu}^{(p-1)}, \\ T_{dd}^{(p)} &= T_{dd}^{(p-1)} [1 - \bar{r}_{du}^{(p-1)} R_{ud}^{(p-1)}]^{-1} \bar{t}_{dd}^{(p)}. \end{aligned} \quad (15a)$$

The S -matrix recursion can be initialized by setting

$$S^{(-1)} = \begin{bmatrix} 1 & 0 \\ 0 & 1 \end{bmatrix}, \quad (16a)$$

or, equivalently, by setting $S^{(0)} = s^{(0)}$.

The form of the factors enclosed by the square brackets in Eq. (15a) is such that the inverse matrices can be readily expanded, at least formally, into a geometrical series in terms of the product of the two reflection matrices. This fact naturally gives rise to the multiple-reflection interpretation of the S -matrix recursion formulas.¹² (It is quite unfortunate that in Ref. 12 the S -matrix algorithm was incorrectly called the R -matrix algorithm.) Because of the elegant form of the inverse matrices, Eqs. (15a) will be called the normalized S -matrix recursion formulas.

Equations (8a)–(16a) constitute the basic ingredients of the S -matrix algorithm. In most grating problems the quantities of interest are the field amplitudes leaving the grating structure in the two outer media, i.e., $u^{(n+1)}$ and $d^{(0)}$. They are simply given by

$$\begin{bmatrix} u^{(n+1)} \\ d^{(0)} \end{bmatrix} = \begin{bmatrix} T_{uu}^{(n)} & R_{ud}^{(n)} \\ R_{du}^{(n)} & T_{dd}^{(n)} \end{bmatrix} \begin{bmatrix} u^{(0)} \\ d^{(n+1)} \end{bmatrix}. \quad (17a)$$

In particular, if there are no incident waves in medium 0 ($u^{(0)} = 0$),

$$\begin{aligned} u^{(n+1)} &= R_{ud}^{(n)} d^{(n+1)}, \\ d^{(0)} &= T_{dd}^{(n)} d^{(n+1)}. \end{aligned} \quad (18a)$$

The numerical stability of the S -matrix algorithm is rooted in the construction of the layer s matrix. The problem-causing, growing exponential function, $\exp(i\lambda_m^{(p)} h_p)$, that was originally in the \tilde{t} matrix, is now inverted in Eq. (13a). Since $s^{(p)}$ is of order $O(1)$, so is $\tilde{s}^{(p)}$. Furthermore, the submatrices of $\tilde{s}^{(p)}$ appear in the recursion formulas only as additive or multiplicative terms. Thus the S matrices remain of order $O(1)$, and the numerical stability of the algorithm is ensured.

4. R-MATRIX ALGORITHM

The R -matrix algorithm uses the trigonometrical basis functions. For any $0 \leq p \leq n$, it seeks a stack R matrix, $R^{(p)}$, that links the fields in layer $p+1$ and medium 0 in this way:

$$\begin{bmatrix} U^{(p+1)} \\ U^{(0)} \end{bmatrix} = R^{(p)} \begin{bmatrix} V^{(p+1)} \\ V^{(0)} \end{bmatrix}. \quad (8b)$$

The R matrix can be physically interpreted as field impedance or field admittance (the ratio of the tangential component of the E field to the tangential component of the H field or its inverse). For example, in TE polarization, because U and V correspond to the E and H fields, respectively, $R^{(p)}$ plays the role of field impedance. An alternative interpretation of Eq. (8b) can be made, with the aid of Fig. 3(b), in terms of currents and voltages in an electrical circuit. Here, if U is identified with the voltages and V with the currents, or vice versa, then $R^{(p)}$ is the electrical impedance or admittance. The concept of impedance has been used previously in modeling grat-

ings that contain multiple planar interfaces but only one periodically modulated interface.¹³

To link the fields in two adjacent layers, we can define an interface r matrix, $r^{(p)}$, and a layer r matrix, $\tilde{r}^{(p)}$, as follows:

$$\begin{bmatrix} U^{(p+1)}(y_p + 0) \\ U^{(p)}(y_p - 0) \end{bmatrix} = r^{(p)} \begin{bmatrix} V^{(p+1)}(y_p + 0) \\ V^{(p)}(y_p - 0) \end{bmatrix}, \quad (10b)$$

$$\begin{bmatrix} U^{(p+1)} \\ U^{(p)} \end{bmatrix} = \tilde{r}^{(p)} \begin{bmatrix} V^{(p+1)} \\ V^{(p)} \end{bmatrix}. \quad (11b)$$

The layer r matrix is related to the interface r matrix by

$$\begin{aligned} \tilde{r}_{11}^{(p)} &= r_{11}^{(p)} - r_{12}^{(p)} \zeta^{(p)} r_{21}^{(p)}, \\ \tilde{r}_{12}^{(p)} &= r_{12}^{(p)} \zeta^{(p)} \eta_m^{(p)} \csc[\lambda_m^{(p)} h_p], \\ \tilde{r}_{21}^{(p)} &= \eta_m^{(p)} \csc[\lambda_m^{(p)} h_p] \zeta^{(p)} r_{21}^{(p)}, \\ \tilde{r}_{22}^{(p)} &= \eta_m^{(p)} \cot[\lambda_m^{(p)} h_p] - \eta_m^{(p)} \csc[\lambda_m^{(p)} h_p] \\ &\quad \times \zeta^{(p)} \eta_m^{(p)} \csc[\lambda_m^{(p)} h_p], \end{aligned} \quad (13b)$$

where

$$\zeta^{(p)} = [r_{22}^{(p)} + \eta_m^{(p)} \cot(\lambda_m^{(p)} h_p)]^{-1}. \quad (13b')$$

For a proof of Eq. (13b), see Appendix A. Here we have excluded the possibility that accidentally $\lambda_m^{(p)} h_p = l\pi$, where l is an integer. The interface r matrix is in turn related to the interface t matrix by

$$r^{(p)} = \begin{bmatrix} t_{11}^{(p)} t_{21}^{(p)-1} & t_{12}^{(p)} - t_{11}^{(p)} t_{21}^{(p)-1} t_{22}^{(p)} \\ t_{21}^{(p)-1} & -t_{21}^{(p)-1} t_{22}^{(p)} \end{bmatrix}. \quad (14b)$$

From Eqs. (13b) and (14b) it is clear that $\tilde{r}^{(p)}$ is of order $O(1)$. Alternatively, we can use the layer t matrix to express the layer r matrix:

$$\tilde{r}^{(p)} = \begin{bmatrix} \tilde{t}_{11}^{(p)} \tilde{t}_{21}^{(p)-1} & \tilde{t}_{12}^{(p)} - \tilde{t}_{11}^{(p)} \tilde{t}_{21}^{(p)-1} \tilde{t}_{22}^{(p)} \\ \tilde{t}_{21}^{(p)-1} & -\tilde{t}_{21}^{(p)-1} \tilde{t}_{22}^{(p)} \end{bmatrix}. \quad (14b')$$

In Eqs. (14b) and (14b') $t_{21}^{(p)}$ and $\tilde{t}_{21}^{(p)}$ are the pivotal submatrices. In some cases it is possible that $t_{21}^{(p)} \equiv 0$, but then $\tilde{t}_{21}^{(p)} \neq 0$. In fact, such a case can be utilized beneficially (see Appendix B).

From Eqs. (8b) and (11b) the set of recursion formulas for the stack R matrix are

$$\begin{aligned} R_{11}^{(p)} &= \tilde{r}_{11}^{(p)} - \tilde{r}_{12}^{(p)} Z^{(p)} \tilde{r}_{21}^{(p)}, \\ R_{12}^{(p)} &= \tilde{r}_{12}^{(p)} Z^{(p)} R_{12}^{(p-1)}, \\ R_{21}^{(p)} &= -R_{21}^{(p-1)} Z^{(p)} \tilde{r}_{21}^{(p)}, \\ R_{22}^{(p)} &= R_{22}^{(p-1)} + R_{21}^{(p-1)} Z^{(p)} R_{12}^{(p-1)}, \end{aligned} \quad (15b)$$

where

$$Z^{(p)} = (\tilde{r}_{22}^{(p)} - R_{11}^{(p-1)})^{-1}. \quad (15b')$$

The R -matrix recursion can be initialized by setting

$$R^{(0)} = \tilde{r}^{(0)}. \quad (16b)$$

Unlike their counterparts in the S -matrix algorithm,

Eqs. (15b) do not readily subject themselves to an intuitive physical interpretation. Nonetheless, to preserve the formal symmetry between the two algorithms, we shall call Eqs. (15b) the normalized R -matrix recursion formulas.

Starting with Eq. (16b), repeated use of Eqs. (15b) until $p = n$ leads to

$$\begin{bmatrix} U^{(n+1)} \\ U^{(0)} \end{bmatrix} = \begin{bmatrix} R_{11}^{(n)} & R_{12}^{(n)} \\ R_{21}^{(n)} & R_{22}^{(n)} \end{bmatrix} \begin{bmatrix} V^{(n+1)} \\ V^{(0)} \end{bmatrix}. \quad (17b)$$

Suppose that $U^{(0)} = u^{(0)} + d^{(0)}$, $V^{(0)} = u^{(0)} - d^{(0)}$, $U^{(n+1)} = u^{(n+1)} + d^{(n+1)}$, and $V^{(n+1)} = u^{(n+1)} - d^{(n+1)}$, which is always possible by definition. Then from Eq. (17b) we get the linear system that determines the out-going diffraction amplitudes in the top and bottom media:

$$\begin{bmatrix} 1 - R_{11}^{(n)} & R_{12}^{(n)} \\ -R_{21}^{(n)} & 1 + R_{22}^{(n)} \end{bmatrix} \begin{bmatrix} u^{(n+1)} \\ d^{(0)} \end{bmatrix} = \begin{bmatrix} -1 - R_{11}^{(n)} & R_{12}^{(n)} \\ -R_{21}^{(n)} & -1 + R_{22}^{(n)} \end{bmatrix} \begin{bmatrix} d^{(n+1)} \\ u^{(0)} \end{bmatrix}. \quad (18b)$$

The R -matrix algorithm is also immune to the numerical difficulties associated with growing exponential functions. This is because the submatrices of $\tilde{r}^{(p)}$ are all of order $O(1)$, and they appear in the recursion formulas Eqs. (15b) and (15b') only as additive and multiplicative terms. The former fact is evident when Eq. (13b) is used to construct the layer r matrices. It is not so obvious if Eqs. (14b') are used, however, in fact, in this case the R -matrix algorithm is only conditionally stable.

It can be shown that Eq. (14b') and Eqs. (13b) are algebraically equivalent. Therefore the submatrix $\tilde{r}_{12}^{(p)}$, as given by Eq. (14b'), should be mathematically proportional to $\csc(\lambda_m^{(p)} h_p)$, which tends to 0 as $m \rightarrow \infty$ and $h_p \rightarrow \infty$. On the other hand, the first term of $\tilde{r}_{12}^{(p)}$ in Eq. (14b') is $\tilde{r}_{12}^{(p)} = t_{11}^{(p)} \eta_m^{(p)} \sin[\lambda_m^{(p)} h_p] + t_{12}^{(p)} \cos[\lambda_m^{(p)} h_p]$, which tends to ∞ . Thus the second term of $\tilde{r}_{12}^{(p)}$ must also tend to ∞ as $m \rightarrow \infty$ and $h_p \rightarrow \infty$. Clearly this mathematical arrangement presents a serious numerical problem. When the absolute values of the imaginary parts of $\lambda_m^{(p)} h_p$ are large, the numerically calculated matrix elements of $\tilde{r}_{12}^{(p)}$ by Eq. (14b') may not be small, as a result of round-off errors. Let $\Lambda^{(p)}$ be the maximum of the absolute values of the imaginary parts of all eigenvalues for a given matrix truncation. As a rule of thumb, when $\exp[\Lambda^{(p)} h_p] \sim 10^{15}$, the numerical problem described above begins to arise (double precision is assumed here). To avoid the problem one has to choose the layer thickness so that $\exp[\Lambda^{(p)} h_p] \ll 10^{15}$. Therefore the R -matrix algorithm is conditionally stable when Eq. (14b') is used. Fortunately, unlike the T -matrix algorithm, here the magnitudes of the exponential functions do not accumulate. Therefore lowering the individual layer thickness is an effective remedy for the numerical instability caused by the use of Eq. (14b').

5. VARIANTS OF IMPLEMENTATION

A. Variation in Matrix Manipulation

In Sections 3 and 4 the S -matrix and R -matrix algorithms were systematically presented. The presentation took

three steps: the definitions and derivations of the layer t matrices, the layer s (or r) matrices, and the stack S (or R) matrices. Although from a theoretical point of view the introduction of the layer t matrices and the layer s (or r) matrices has made the presentation systematic, from a practical point of view the use of one of the two kinds of layer matrices can be eliminated, as demonstrated below.

The S -matrix recursion can be accomplished by use of the t matrices directly, without the layer s matrices. From Eqs. (5a), (6), and (9a) we can easily derive a set of nonnormalized S -matrix recursion formulas by using the interface t matrix:

$$\begin{aligned} T_{uu}^{(p)} &= [t_{11}^{(p)} - R_{ud}^{(p)} t_{21}^{(p)}] \phi_+^{(p)} T_{uu}^{(p-1)}, \\ R_{ud}^{(p)} &= [t_{12}^{(p)} + t_{11}^{(p)} \Omega^{(p)}] [t_{22}^{(p)} + t_{21}^{(p)} \Omega^{(p)}]^{-1}, \\ R_{du}^{(p)} &= R_{du}^{(p-1)} - T_{dd}^{(p-1)} t_{21}^{(p)} \phi_-^{(p)} T_{uu}^{(p-1)}, \\ T_{dd}^{(p)} &= T_{dd}^{(p-1)} \phi_-^{(p-1)-1} [t_{22}^{(p)} + t_{21}^{(p)} \Omega^{(p)}]^{-1}, \end{aligned} \quad (19a)$$

where

$$\Omega^{(p)} = \phi_+^{(p)} R_{ud}^{(p-1)} \phi_-^{(p-1)-1}, \quad (19a')$$

and $\phi_{\pm}^{(p)}$ are the two diagonal submatrices in Eq. (4a). Of course, Eqs. (19a) and (15a) are algebraically equivalent. Note that the above equations have been written in terms of the interface t matrices, instead of the layer t matrices, and the appearance of $\phi_{\pm}^{(p)}$ has been arranged properly so that there are no exponentially growing functions in the formulas. This measure avoids possible numerical overflow and ensures numerical stability of the S -matrix algorithm.

If we set $\phi_{\pm}^{(p)} = 1$ in Eqs. (19a) and (19a') and replace all interface t submatrices by layer t submatrices, we obtain the nonnormalized S -matrix recursion formulas by using the layer t matrix:

$$\begin{aligned} T_{uu}^{(p)} &= [t_{11}^{(p)} - R_{ud}^{(p)} t_{21}^{(p)}] T_{uu}^{(p-1)}, \\ R_{ud}^{(p)} &= [t_{12}^{(p)} + t_{11}^{(p)} R_{ud}^{(p-1)}] [t_{22}^{(p)} + t_{21}^{(p)} R_{ud}^{(p-1)}]^{-1}, \\ R_{du}^{(p)} &= R_{du}^{(p-1)} - T_{dd}^{(p-1)} t_{21}^{(p)} T_{uu}^{(p-1)}, \\ T_{dd}^{(p)} &= T_{dd}^{(p-1)} [t_{22}^{(p)} + t_{21}^{(p)} R_{ud}^{(p-1)}]^{-1}. \end{aligned} \quad (20a)$$

The use of this set of recursion formulas should be avoided whenever possible, because the matrix to be inverted is a sum of an exponentially growing matrix and an exponentially decaying matrix.

The R -matrix recursion can also be accomplished with use of the t matrices directly, without the layer r matrices. From Eqs. (5b), (6), and (8b) we can easily derive a set of nonnormalized R -matrix recursion formulas by using the layer t matrix:

$$\begin{aligned} R_{11}^{(p)} &= [t_{12}^{(p)} + t_{11}^{(p)} R_{11}^{(p-1)}] [t_{22}^{(p)} + t_{21}^{(p)} R_{11}^{(p-1)}]^{-1}, \\ R_{12}^{(p)} &= [t_{11}^{(p)} - R_{11}^{(p)} t_{21}^{(p)}] R_{12}^{(p-1)}, \\ R_{21}^{(p)} &= R_{21}^{(p-1)} [t_{22}^{(p)} + t_{21}^{(p)} R_{11}^{(p-1)}]^{-1}, \\ R_{22}^{(p)} &= R_{22}^{(p-1)} - R_{21}^{(p)} t_{21}^{(p)} R_{12}^{(p-1)}. \end{aligned} \quad (20b)$$

Since Eqs. (20b) are algebraically equivalent to Eqs. (15b),

the R matrices obtained this way are mathematically of order $O(1)$. Numerically, however, devastating round-off errors could occur if the numerical layer thicknesses are set too high. The reason is the same as the one given at the end of Section 4 for the possible numerical instability resulting from the use of Eq. (14b'). Specifically, the expression of $R_{12}^{(p)}$ in Eqs. (20b) is of type $\infty - \infty = O(1)$. Thus Eqs. (20b) also give a conditional stable implementation of the R -matrix algorithm. The unconditional

$$\begin{bmatrix} a_{uu} & a_{ud} \\ a_{du} & a_{dd} \end{bmatrix} * \begin{bmatrix} b_{uu} & b_{ud} \\ b_{du} & b_{dd} \end{bmatrix} = \begin{bmatrix} b_{uu}(1 - a_{ud}b_{du})^{-1}a_{uu} & b_{ud} + b_{uu}a_{ud}(1 - b_{du}a_{ud})^{-1}b_{dd} \\ a_{du} + a_{dd}b_{du}(1 - a_{ud}b_{du})^{-1}a_{uu} & a_{dd}(1 - b_{du}a_{ud})^{-1}b_{dd} \end{bmatrix}, \quad (23a)$$

stable, nonnormalized R -matrix recursion formulas obtained by using the interface t matrix are given in Appendix C.

We recall that in Subsection 2.C we formally derived the layer t matrix from the boundary equation, Eq. (2a) or Eq. (2b). In fact, in at least two important cases Eq. (5a) or Eq. (5b) is obtained without the aid of Eq. (2a) or Eq. (2b). The first case is the classical modal method in which matrix $t^{(p)}$ is obtained directly by projecting the functional boundary equations onto a natural basis function set,⁷ and the second case is the differential method in which matrix $\tilde{t}^{(p)}$ is obtained from a numerical integration procedure.⁹ In these cases the use of the non-normalized recursion formulas may be beneficial because they require fewer matrix operations.

In the C method and the coupled-wave method the boundary equations (2a) or (2b) are an integral step of the numerical treatment. In this case we can bypass the t matrix and derive the s (or r) matrix directly from the boundary equations. Writing the two W matrices in Eq. (2a) in a two-by-two form, and rearranging the terms slightly, we have

$$\begin{bmatrix} W_{11}^{(p+1)} & -W_{12}^{(p)} \\ W_{21}^{(p+1)} & -W_{22}^{(p)} \end{bmatrix} \begin{bmatrix} u^{(p+1)}(y_p + 0) \\ d^{(p)}(y_p - 0) \end{bmatrix} = \begin{bmatrix} W_{11}^{(p)} & -W_{12}^{(p+1)} \\ W_{21}^{(p)} & -W_{22}^{(p+1)} \end{bmatrix} \begin{bmatrix} u^{(p)}(y_p - 0) \\ d^{(p+1)}(y_p + 0) \end{bmatrix}. \quad (21a)$$

Therefore from Eq. (10a),

$$s^{(p)} = \begin{bmatrix} W_{11}^{(p+1)} & -W_{12}^{(p)} \\ W_{21}^{(p+1)} & -W_{22}^{(p)} \end{bmatrix}^{-1} \begin{bmatrix} W_{11}^{(p)} & -W_{12}^{(p+1)} \\ W_{21}^{(p)} & -W_{22}^{(p+1)} \end{bmatrix}. \quad (22a)$$

The layer s matrix, $\tilde{s}^{(p)}$, then follows immediately from Eq. (13a). Similarly the interface r matrix, $r^{(p)}$, can be derived directly from boundary equation (2b); i.e.,

$$r^{(p)} = \begin{bmatrix} W_{11}^{(p+1)} & -W_{11}^{(p)} \\ W_{21}^{(p+1)} & -W_{21}^{(p)} \end{bmatrix}^{-1} \begin{bmatrix} -W_{12}^{(p+1)} & W_{12}^{(p)} \\ -W_{22}^{(p+1)} & W_{22}^{(p)} \end{bmatrix}. \quad (22b)$$

The layer r matrix, $\tilde{r}^{(p)}$, then follows immediately from Eq. (13b).

B. Variation in Recursion Order

The S -matrix and R -matrix recursions do not have to be performed in the order indicated in Sections 3 and 4. In other words, one does not have to start the calculation from medium 0 and work step by step up to medium $n + 1$. For the normalized recursions this point can be best illustrated by the use of Redheffer's start product.²⁰ Let a , b , and c be $2N \times 2N$ matrices. Then the star product of a and b , in the S -matrix algorithm, is defined as

$$\begin{bmatrix} a_{11} & a_{12} \\ a_{21} & a_{22} \end{bmatrix} * \begin{bmatrix} b_{11} & b_{12} \\ b_{21} & b_{22} \end{bmatrix} = \begin{bmatrix} b_{11} - b_{12}(b_{22} - a_{11})^{-1}b_{21} & b_{12}(b_{22} - a_{11})^{-1}a_{12} \\ -a_{21}(b_{22} - a_{11})^{-1}b_{21} & a_{22} + a_{21}(b_{22} - a_{11})^{-1}a_{12} \end{bmatrix}. \quad (23b)$$

It can be shown that the star multiplications are associative, i.e., that

$$a * (b * c) = (a * b) * c, \quad (24a)$$

$$a * (b * c) = (a * b) * c. \quad (24b)$$

In the remainder of this section, for simplicity, I will mention only the S -matrix recursion. The results for the R -matrix recursion can be obtained by obvious substitutions.

In terms of star products, the S -matrix algorithm can be succinctly expressed as

$$S^{(n)} = \{ \dots [(\tilde{s}^{(0)} * \tilde{s}^{(1)}) * \tilde{s}^{(2)}] * \dots * \tilde{s}^{(n)} \}. \quad (25a)$$

However, because of the associativity of the star multiplication, the product can be regrouped as follows:

$$S^{(n)} = \tilde{s}^{(0)} * \{ \dots * [\tilde{s}^{(n-2)} * (\tilde{s}^{(n-1)} * \tilde{s}^{(n)})] * \dots \}. \quad (26a)$$

Equation (26a) describes the S -matrix recursion in the reverse order, starting from medium $n + 1$ and moving downward to medium 0.

The associativity of the S -matrix recursion can be used advantageously to save computation effort or to increase computation speed. Suppose that a large number of calculations are to be carried out for a grating with a varying parameter that affects only the j th layer, for fixed j . Then the S -matrix recursion can be performed like this:

$$S^{(n)} = [\tilde{s}^{(0)} * \dots * \tilde{s}^{(j-1)}] * \tilde{s}^{(j)} * [\tilde{s}^{(j+1)} * \dots * \tilde{s}^{(n)}], \quad (27a)$$

where the two recursions inside the square brackets are performed just once and then are used repeatedly to form a star product with the changing $\tilde{s}^{(j)}$. If the grating calculation is done on a computer capable of parallel pro-

cessing, then the S matrices can be grouped pairwise to increase the computation speed.

6. COMPARISONS

Having systematically addressed the S -matrix and R -matrix algorithms and their variants, we are now ready to make some comparisons. As mentioned in Sections 3 and 4, the S matrices are related to the physical concept of reflection and transmission, and the R matrices are related to the physical concept of impedance and admittance. Furthermore, the normalized S -matrix recursion formulas can be readily interpreted in terms of multiple reflections, but the R -matrix recursion formulas and the nonnormalized S -matrix recursion formulas are not easily interpreted in physical terms. In what follows we compare the numerical stabilities and efficiencies of the two algorithms.

A. Numerical Stabilities

Both the S -matrix and R -matrix algorithms are inherently stable because the S matrices and the R matrices are both mathematically of order $O(1)$. However, there are subtle numerical differences between them. In general the S -matrix algorithm is much easier to work with than the R matrix algorithm.

The implementation of the S -matrix algorithm is mostly worry free (but see Subsection 7.D), thanks to its use of the exponential basis functions. All s and S matrices are of order $O(1)$, not only mathematically but also numerically [we assume that Eqs. (20a) are not used]. Thus there is no limit in layer thickness. The possibility of numerical overflow associated with the exponential functions is eliminated because only the decreasing exponential functions are evaluated. Underflow can happen, but it is not a problem for most compilers. Additionally, the occurrence of $\lambda_m^{(p)} h_p = l\pi$ is not a problem at all.

The implementation of the R -matrix algorithm requires special treatment. Although all r and R matrices are of order $O(1)$ mathematically, they may not be so numerically. When the factorization of the layer l matrix into the product of the interface l matrix and the diagonal matrix ϕ is possible, one should use Eqs. (C1) and (C2) below to perform the nonnormalized recursion or use Eqs. (13b) to compute $\tilde{r}^{(p)}$ if the normalized recursion is to be used. When the factorization is impossible, as is the case for the differential method, the numerical layer thicknesses should be kept sufficiently low that the computation of $\tilde{r}_{12}^{(p)}$ by Eq. (14b') or of $R_{12}^{(p)}$ by Eq. (20b) will not suffer significant loss of accuracy. There is also a minor technical complication. Functions \cot and \csc that admit a complex argument are not intrinsic functions in most compilers. Thus the programmer has to write \cot and \csc as user-defined functions, using either the sine and cosine functions or the exponential functions. In doing so, care has to be taken to avoid overflow. In principle, the accidental occurrence of $\lambda_m^{(p)} h_p = l\pi$ is a problem for the R -matrix algorithm. In practice, it is highly unlikely that the equality holds for $l \neq 0$ with high precision; therefore the singularity never poses serious numerical problems. Of course, one should judiciously avoid $h_p = 0$, which is an uninteresting case, anyway.

B. Numerical Efficiencies

In this subsection we consider the numerical efficiencies of different variants of the S -matrix and R -matrix algorithms. More specifically, we estimate the number of algebraic operations that each variant takes to compute the outgoing diffraction amplitudes $u^{(n+1)}$ and $d^{(0)}$, assuming that the W matrices in the boundary equations have been obtained.

As is evident from the presentations in Sections 3 and 4, after the S -matrix recursion is completed, $u^{(n+1)}$ and $d^{(0)}$ are readily given in a solved form. However, with the R -matrix algorithm the completion of the R -matrix recursion only gives a system of linear equations that has yet to be solved to yield $u^{(n+1)}$ and $d^{(0)}$. This initial comparison is already in favor of the S -matrix algorithm.

We now take a closer look at the structure of the matrix recursion formulas. We say that a subset of the four submatrices of $S^{(p)}$ is a closed set with respect to the S -matrix recursion if every element of the set is determined by the elements in the same set. Thus $S^{(p)}$ has four closed proper subsets:

$$\{R_{ud}^{(p)}\}, \quad \{R_{ud}^{(p)}, T_{dd}^{(p)}\}, \quad \{R_{ud}^{(p)}, T_{uu}^{(p)}\}, \\ \{R_{ud}^{(p)}, T_{uu}^{(p)}, T_{dd}^{(p)}\}. \quad (28a)$$

If there are incident plane waves in both media 0 and $n+1$, then from Eq. (17a) the S -matrix recursion of all four submatrices has to be performed. Suppose that $u^{(0)} = 0$; then only the recursion of $\{R_{ud}^{(p)}, T_{dd}^{(p)}\}$ is necessary if both $u^{(n+1)}$ and $d^{(0)}$ are needed, and only the recursion of $R_{ud}^{(p)}$ is necessary if only $u^{(n+1)}$ is needed. We call the recursions above the full, half, and quarter S -matrix recursions, respectively.

Similarly, $R^{(p)}$ also has four closed proper subsets:

$$\{R_{11}^{(p)}\}, \quad \{R_{11}^{(p)}, R_{12}^{(p)}\}, \quad \{R_{11}^{(p)}, R_{21}^{(p)}\}, \\ \{R_{11}^{(p)}, R_{12}^{(p)}, R_{21}^{(p)}\}. \quad (28b)$$

With the R -matrix algorithm, if both $u^{(n+1)}$ and $d^{(0)}$ are needed, the full matrix recursion has to be performed even when $u^{(0)} = 0$. If $d^{(0)}$ is not needed and $u^{(0)} = 0$, then quarter R -matrix recursion with $R_{11}^{(p)}$ is possible, but the R matrix has to be initialized by

$$R^{(-1)} = \begin{bmatrix} 1 & 0 \\ 0 & -1 \end{bmatrix}. \quad (29b)$$

With this initialization, $R_{12}^{(p)} = R_{21}^{(p)} = 0$ and $R_{22}^{(p)} = -1$ for all p .

Finally, we shall provide operation counts per grating layer for the variants of the two recursive matrix algorithms that have been presented in this paper. The operation counts will be given in units of flops.²¹ The counts do not include the effort in assembling the W matrices and in solving the final linear system to yield $u^{(n+1)}$ and $d^{(0)}$. For convenience, we shall consider only the operations that are proportional to N^3 , where N is the truncation order, the dimension of the submatrices. The method of counting is based on well-established rules²¹: suppose that A , B , and C are $N \times N$ nonsparse matrices.

Table 1. Operation Counts (in N^3 Flops) per Grating Layer for Different Variants of the S-Matrix and R-Matrix Algorithms

Algorithm Number	Algorithm	Stability	Operation Counts		
			Full	Half	Quarter
1a	$W \rightarrow t \rightarrow s \rightarrow \bar{s} \rightarrow S$	Unconditional	76/3	20	19
2a	$W \rightarrow t \rightarrow S$	Unconditional	19	15	14
3a	$W \rightarrow s \rightarrow \bar{s} \rightarrow S$	Unconditional	64/3	16	15
4a	$W \rightarrow \bar{t} \rightarrow S$	Conditional	19	15	14
1b	$W \rightarrow t \rightarrow r \rightarrow \bar{r} \rightarrow R$	Unconditional	25	—	21
2b	$W \rightarrow t \rightarrow R$	Unconditional	28	—	15
3b	$W \rightarrow r \rightarrow \bar{r} \rightarrow R$	Unconditional	21	—	17
4b	$W \rightarrow \bar{t} \rightarrow \bar{r} \rightarrow R$	Conditional	21	—	17
5b	$W \rightarrow \bar{t} \rightarrow R$	Conditional	19	—	14

ces; then $AB + C$, A^{-1} , and $A^{-1}B + C$ take N^3 , N^3 , and $(4/3)N^3$ flops, respectively.

The results are summarized in Table 1 where implementation variants of the S-matrix and R-matrix algorithms that have been described in Sections 3, 4, and 5 are represented symbolically. For example, $W \rightarrow t \rightarrow S$ represents the variant of the S-matrix algorithm that uses Eq. (7) to compute the interface t matrix and then uses Eqs. (19a) to perform the S-matrix recursion. The broken arrows indicate that in some grating models the t matrices are obtained without using the W matrices. In this case, $(32/3)N^3$ flops should be subtracted from the operation counts in Table 1. The subheadings of the last three columns stand for full-, half-, and quarter-matrix recursions, respectively. Since the half-matrix recursion of the R matrices serves no useful purpose, the corresponding operation counts are not given. Clearly, algorithms 2a and 3a are the most efficient, assuming that we start with the W matrices.

7. REMARKS

A. Algorithm of Chateau and Hugonin

It is easy to see that the algorithm proposed by Chateau and Hugonin,⁸ except for the notational differences, is algorithm 2a in Table 1 for the special case in which $u^{(0)} = 0$. It is one of the most efficient variants of the general S-matrix algorithm, but it can be slightly improved. In Ref. 8 each of the three factors of the layer t matrix [see Eqs. (6) and (7)] is passed through the recursion formula separately. So the operation count, including the inversion of $W^{(p+1)}$, is $(50/3)N^3$ for the half-recursion. In comparison, the use of product $t = W^{(p+1)-1}W^{(p)}$ in Eq. (19a) costs $15N^3$ flops.

B. R-Matrix Algorithm and Differential Method

For the differential method it is natural to use the R-matrix algorithm because here the $U-V$ basis is the natural basis. The factorization of the layer t matrices is unavailable in the differential method, so the application of the R-matrix starts with the layer t matrices. As explained in Sections 4 and 5, use of the \bar{t} matrix in the R-matrix algorithm makes the stability of the algorithm conditional. Although the modal methods were assumed when we analyzed the cause of numerical instability of Eq. (14b'), the conclusion applies to the differential method as well, because the basis functions are asymptotically the same in the two cases.

The first few rows of Tables 1, 2, and 3 in Ref. 9 clearly indicate that if the numerical layer thicknesses are not kept low, the R-matrix algorithm fails when applied to the differential method.

The R-matrix algorithm that is used in Ref. 9 is algorithm 4b in Table 1 of this paper, which takes $(31/3)N^3$ flops per layer for the full-matrix recursion. It can be improved slightly by using algorithm 5b, which takes $(25/3)N^3$ flops per layer. Instead, if the $u-d$ basis functions and algorithm 4a are used, significant improvement can be achieved. The operation count for the S-matrix algorithm is only $(13/3)N^3$ flops per layer for the half-matrix recursion. Furthermore, the extra work of solving the final system of linear equations, Eq. (17b), is avoided.

C. R-Matrix Algorithm and Classical Modal Method

In the classical modal method,⁷ thanks to the orthogonality of the modal functions and the fact that the pivotal submatrix $t_{21}^{(p)} = 0$, not only are the t matrices obtained analytically without the W matrices, but the r matrices can also be determined analytically from the t matrices without numerical inversion of the pivotal submatrix. The result is the most efficient variant of the R-matrix algorithm, which can be symbolized simply as $\bar{r} \rightarrow R$. Only one of the four submatrices of $\bar{r}^{(p)}$ takes N^3 flops to construct; the rest involve only N^2 processes. Thus the overall operation counts are only $(22/3)N^3$ and $(10/3)N^3$ per layer for the full- and quarter-matrix recursions, respectively.

D. S-Matrix Algorithm and Classical Modal Method

The S-matrix algorithm can be applied to the classical modal method, the most efficient variant being algorithm 2a of Table 1. The combination of the S-matrix algorithm and the classical modal method has a peculiar problem, which I shall describe below.

In the classical modal method, the t matrices that use the exponential basis functions can also be obtained analytically without the W matrices, but the s matrices in general cannot. Without going into any detail, suffice it to say that the elements of $t^{(p)}$ at a numerical interface are all of the form

$$\int \psi_i^{(p+1)}(x) f_p(x) \psi_n^{(p)}(x) dx. \quad (30)$$

where the integration is over one grating period, $\psi_i^{(p+1)}$

and $\psi_n^{(p)}$ are modal functions in layers $p+1$ and p , respectively, and f_p is a function that depends only on the permittivity distribution of the two layers. In what follows, we consider the evaluation of Eq. (30) under a specific set of conditions: (1) the permittivity distributions in two adjacent layers are symmetrical with respect to the origin of the x axis, (2) the grating is in the first-order Littrow mount, and (3) $N = 2M + 1$, where M is a natural number. Under condition (1), f_p is a symmetrical function. Under condition (2), $\psi_l^{(p+1)}$ and $\psi_n^{(p)}$ are either symmetrical or antisymmetrical functions. Thus if integers l and n correspond to modal functions of different parities, the corresponding t matrix element is identically zero. In the classical modal method, one normally indexes the eigenvalues in the order of increasing absolute values. Let $N_e^{(p)}$ and $N_o^{(p)}$ be the numbers of even and odd eigenvalues, respectively. Numerical experiments show that, under condition (2) and for a given truncation order $N = N_e^{(p)} + N_o^{(p)}$, $N_e^{(p)}$ and $N_o^{(p)}$ never differ by more than 1. Thus under condition (3), either $N_e^{(p)} = M$ and $N_o^{(p)} = M + 1$, or $N_e^{(p)} = M + 1$ and $N_o^{(p)} = M$. It can be easily shown that if $N_e^{(p)} \neq N_e^{(p+1)}$ then all submatrices of $t^{(p)}$, in particular the pivotal submatrix $t_{22}^{(p)}$, are mathematically singular. Numerically, the condition $N_e^{(p)} \neq N_e^{(p+1)}$ does often occur; therefore algorithm 1a of Table 1 cannot be applied to the classical modal method when conditions (1), (2), and (3) are met simultaneously. It can be verified numerically that the matrix sum that is to be inverted in Eqs. (19a) sometimes becomes numerically ill-conditioned under the above three conditions; therefore algorithm 2a fails too, even though it does not involve the inversion of the pivotal submatrix $t_{22}^{(p)}$.

Fortunately, the singular matrix problem described above can be easily avoided by the use of an even truncation order. If $N = 2M$, then the characteristics of the eigenvalue distribution automatically guarantee that $N_e^{(p)} = N_o^{(p)} = M$.

Another interesting difference between the R -matrix algorithm and the S -matrix algorithm, as they are applied to the classical modal method, is that the law of energy conservation (in the case of dielectric gratings) is satisfied automatically by the former, but it is satisfied only with increasing truncation orders by the latter.

E. Other Possibilities

The essence of the R -matrix and S -matrix algorithms is to avoid the presence of the growing exponential functions in the matrix manipulations. In this spirit, several other stable algorithms have recently been presented in the literature. For example, Montiel and Nevière⁹ presented an algorithm that they called the R' -matrix algorithm. In view of the current paper, it can be considered an S -matrix algorithm that uses the U - V basis functions. In Ref. 10 the R -matrix algorithm was used with the exponential basis functions (maybe it can be called the S' -matrix algorithm?). The scattering-matrix approach of Cotter *et al.*¹¹ is essentially algorithm 2a of Table 1, except that their t matrix is the inverse of the t matrix in this paper. Clearly there are many other possibilities, but it is pointless to enumerate all of them.

8. SUMMARY

The mathematical formulations of the S -matrix and R -matrix algorithms have been systematically presented. The presentation is given in a unified fashion, independent of underlying grating models, grating geometries, and grating mountings. The physical interpretations of the algorithms are illustrated. In addition, many variants of the algorithms are presented and their numerical stabilities and efficiencies analyzed.

The S -matrix and R -matrix algorithms are inherently stable because they avoid the appearance of the exponentially growing submatrices in the recursion formulas. However, to further ensure that the algorithms be unconditionally stable, effort should be made to avoid the exponentially growing submatrices in the intermediate steps, i.e., in the calculation of the layer s or r submatrices. Whenever the factorization, as given in Eq. (6), of the layer t matrix is possible, the interface t matrix should be used directly in the constructions of layer s (or r) matrix or in the nonnormalized S -matrix (or R -matrix) recursion. When factorization is impossible, the S -matrix and R -matrix algorithms are stable under the condition that the layer thicknesses and the truncation order be kept low, as quantified at the end of Section 4.

The comparative study of the two matrix algorithms presented here seems to favor the S -matrix algorithm. The physical interpretation of the S matrix in terms of reflections and transmissions is more intuitive than that of the R matrix in terms of the impedance and admittance. The exponential basis functions adopted by the S -matrix algorithm are numerically much easier to handle than the trigonometrical basis functions adopted by the R matrix algorithm. Based on the operation counts, the S -matrix algorithm is more efficient than the R -matrix algorithm.

Many implementation variants of the algorithms are presented in this paper. The variants that use all intermediate matrices, algorithms 1a and 1b in Table 1, are the least efficient ones. They have only pedagogical value. The variants that bypass some of the intermediate matrices, for example, algorithms 2a, 3a, and 2b, are the most efficient ones. However, as exemplified in Section 7, which algorithm and variant are more efficient often depends on the grating model being used. It is the hope of the author that the information provided here will enable the reader to apply the most efficient algorithm to the grating model at his or her disposal.

APPENDIX A

To derive Eq. (13b), let us imagine that layer p is a sum of two layers. The first layer has zero thickness, with the layer t and r matrices given by Eqs. (7) and (14b), respectively. The second layer has thickness h_p , but it does not cross a material boundary. Its equivalent layer t matrix is just $\phi^{(p)}$, given by Eq. (4b). Denoting the equivalent layer r matrix corresponding to $\phi^{(p)}$ by $r^{(p)}$ from Eq. (14b) we have

$$r^{(p)} = \begin{bmatrix} -\eta_m^{(p)} \cot(\lambda_m^{(p)} h_p) & \eta_m^{(p)} \csc(\lambda_m^{(p)} h_p) \\ -\eta_m^{(p)} \csc(\lambda_m^{(p)} h_p) & \eta_m^{(p)} \cot(\lambda_m^{(p)} h_p) \end{bmatrix}. \quad (\text{A1})$$

Equations (15b) can be viewed as a set of rules that

combine matrix $\tilde{r}^{(p)}$ in relation

$$\begin{bmatrix} U^{(p+1)} \\ U^{(p)} \end{bmatrix} = \tilde{r}^{(p)} \begin{bmatrix} V^{(p+1)} \\ V^{(p)} \end{bmatrix} \quad (\text{A2})$$

and matrix $R^{(p-1)}$ in relation

$$\begin{bmatrix} U^{(p)} \\ U^{(0)} \end{bmatrix} = R^{(p-1)} \begin{bmatrix} V^{(p)} \\ V^{(0)} \end{bmatrix} \quad (\text{A3})$$

to obtain matrix $R^{(p)}$ in relation

$$\begin{bmatrix} U^{(p+1)} \\ U^{(0)} \end{bmatrix} = \hat{R}^{(p)} \begin{bmatrix} V^{(p+1)} \\ V^{(0)} \end{bmatrix}. \quad (\text{A4})$$

Here we have

$$\begin{bmatrix} U^{(p+1)}(y_p + 0) \\ U^{(p)}(y_p - 0) \end{bmatrix} = r^{(p)} \begin{bmatrix} V^{(p+1)}(y_p + 0) \\ V^{(p)}(y_p - 0) \end{bmatrix}, \quad (\text{A5})$$

$$\begin{bmatrix} U^{(p)}(y_p - 0) \\ U^{(p)}(y_{p-1} + 0) \end{bmatrix} = \tilde{r}^{(p)} \begin{bmatrix} V^{(p)}(y_p - 0) \\ V^{(p)}(y_{p-1} + 0) \end{bmatrix}. \quad (\text{A6})$$

and what we want is the matrix in

$$\begin{bmatrix} U^{(p+1)}(y_p + 0) \\ U^{(p)}(y_{p-1} + 0) \end{bmatrix} = \tilde{r}^{(p)} \begin{bmatrix} V^{(p+1)}(y_p + 0) \\ V^{(p)}(y_{p-1} + 0) \end{bmatrix}. \quad (\text{A7})$$

Through comparison of Eqs. (A2)–(A4) with Eqs. (A5)–(A7), it is evident that the two sets of equations have identical algebraic structures. Therefore Eqs. (13b) can be obtained from Eqs. (15b) provided that $r^{(p)}$, $\tilde{r}^{(p)}$, and $\tilde{r}^{(p)}$ are identified with $\tilde{r}^{(p)}$, $R^{(p-1)}$, and $R^{(p)}$, respectively.

APPENDIX B

When $t_{21}^{(p)} = 0$, which happens in the classical modal method, Eq. (14b) cannot be used to compute $r^{(p)}$, but in this case for sure $t_{22}^{(p)} \neq 0$. Suppose that $t_{22}^{(p)}$ is nonsingular and $\lambda_m^{(p)} h_p \neq \pi$, then Eq. (14b') can be used to derive the layer r matrix. After some simple algebra, we have

$$\tilde{r}^{(p)} = \begin{bmatrix} [t_{12}^{(p)} - t_{11}^{(p)} \eta_m^{(p)} \cot(\lambda_m^{(p)} h_p)] t_{22}^{(p)-1} & t_{11}^{(p)} \eta_m^{(p)} \csc(\lambda_m^{(p)} h_p) \\ -\eta_m^{(p)} \csc(\lambda_m^{(p)} h_p) t_{22}^{(p)-1} & \eta_m^{(p)} \cot(\lambda_m^{(p)} h_p) \end{bmatrix}. \quad (\text{B1})$$

This expression of $\tilde{r}^{(p)}$, like Eqs. (13b), contains no exponentially growing functions, and therefore is suitable for the unconditionally stable R -matrix recursion.

APPENDIX C

Similarly to the treatment in Appendix A, we consider that each of the two factors in Eq. (6) corresponds to a layer, one with zero thickness and the other with the full thickness h_p . Substituting $\phi^{(p)}$ for $\tilde{r}^{(p)}$ in Eqs. (20b), and making some simple algebraic rearrangement, we obtain

an intermediate R matrix, $\hat{R}^{(p)}$, which is given by

$$\begin{aligned} \hat{R}_{11}^{(p)} &= -\eta_m^{(p)} \cot(\lambda_m^{(p)} h_p) + \eta_m^{(p)} \csc(\lambda_m^{(p)} h_p) \\ &\quad \times \omega^{(p)} \eta_m^{(p)} \csc(\lambda_m^{(p)} h_p), \\ \hat{R}_{12}^{(p)} &= \eta_m^{(p)} \csc(\lambda_m^{(p)} h_p) \omega^{(p)} R_{12}^{(p-1)}, \\ \hat{R}_{21}^{(p)} &= R_{21}^{(p-1)} \omega^{(p)} \eta_m^{(p)} \csc(\lambda_m^{(p)} h_p), \\ \hat{R}_{22}^{(p)} &= R_{22}^{(p-1)} + R_{21}^{(p-1)} \omega^{(p)} R_{12}^{(p-1)}, \end{aligned} \quad (\text{C1})$$

where

$$\omega^{(p)} = [\eta_m^{(p)} \cot(\lambda_m^{(p)} h_p) - R_{11}^{(p-1)}]^{-1}. \quad (\text{C1}')$$

Clearly, all submatrices of $\hat{R}^{(p)}$ are of order $O(1)$ and numerically stable. To complete the nonnormalized R -matrix recursion using the interface t matrix, we need only to use Eqs. (20b) again, this time replacing $R^{(p-1)}$ by $\hat{R}^{(p)}$ and $\tilde{r}^{(p)}$ by $t^{(p)}$. The result is

$$\begin{aligned} R_{11}^{(p)} &= [t_{12}^{(p)} + t_{11}^{(p)} \hat{R}_{11}^{(p)}] [t_{22}^{(p)} + t_{21}^{(p)} \hat{R}_{11}^{(p)}]^{-1}, \\ R_{12}^{(p)} &= [t_{11}^{(p)} - R_{11}^{(p)} t_{21}^{(p)}] \hat{R}_{12}^{(p)}, \\ R_{21}^{(p)} &= \hat{R}_{21}^{(p)} [t_{22}^{(p)} + t_{21}^{(p)} \hat{R}_{11}^{(p)}]^{-1}, \\ R_{22}^{(p)} &= \hat{R}_{22}^{(p)} - R_{21}^{(p)} t_{21}^{(p)} \hat{R}_{12}^{(p)}. \end{aligned} \quad (\text{C2})$$

ACKNOWLEDGMENTS

This research was supported by the Optical Data Storage Center, University of Arizona, and by the advanced Technology Program of the U.S. Department of Commerce through a grant to the National Storage Industry Consortium.

REFERENCES AND NOTES

1. L. Li and J. Hirsch, "All-dielectric high-efficiency reflection gratings made with multilayer thin film coatings," *Opt. Lett.* **20**, 1349–1351 (1995).
2. C. Heine and R. H. Morf, "Submicrometer gratings for solar energy applications," *Appl. Opt.* **34**, 2476–2482 (1995).
3. M. Nevière, "Bragg–Fresnel multilayer gratings: electromagnetic theory," *J. Opt. Soc. Am. A* **11**, 1835–1845 (1994).
4. D. Maystre, "Electromagnetic study of photonic band gaps," *Pure Appl. Opt.* **3**, 975–993 (1994).
5. D. M. Pai and K. A. Awada, "Analysis of dielectric gratings of arbitrary profiles and thicknesses," *J. Opt. Soc. Am. A* **8**, 755–762 (1991).
6. L. F. DeSandro and J. M. Elson, "Extinction-theorem analysis of diffraction anomalies in overcoated gratings," *J. Opt. Soc. Am. A* **8**, 763–777 (1991).
7. L. Li, "Multilayer modal method for diffraction gratings of arbitrary profile, depth, and permittivity," *J. Opt. Soc. Am. A* **10**, 2581–2591 (1993).
8. N. Chateau and J. P. Hugonin, "Algorithm for the rigorous coupled-wave analysis of grating diffraction," *J. Opt. Soc. Am. A* **11**, 1321–1331 (1994).
9. F. Montiel and M. Nevière, "Differential theory of gratings: extension to deep gratings of arbitrary profile and permittivity through the R -matrix propagation algorithm," *J. Opt. Soc. Am. A* **11**, 3241–3250 (1994).
10. L. Li, "Multilayer-coated diffraction gratings: differential method of Chandezon et al. revisited," *J. Opt. Soc. Am. A* **11**, 2816–2828 (1994).
11. N. P. K. Cotter, T. W. Preist, and J. R. Sambles, "Scattering-matrix approach to multilayer diffraction," *J. Opt. Soc. Am. A* **12**, 1097–1103 (1995).

12. L. Li, "Bremmer series, R-matrix propagation algorithm, and numerical modeling of diffraction gratings," *J. Opt. Soc. Am. A* 11, 2829-2836 (1994).
13. M. G. Moharam, D. A. Pommet, E. B. Grann, and T. K. Gaylord, "Stable implementation of the rigorous coupled-wave analysis for surface-relief gratings: enhanced transmission matrix approach," *J. Opt. Soc. Am. A* 12, 1077-1086 (1995).
14. M. G. Moharam and T. K. Gaylord, "Diffraction analysis of dielectric surface-relief gratings," *J. Opt. Soc. Am.* 72, 1385-1392 (1982).
15. R. H. Morf, "Exponentially convergent and numerically efficient solution of Maxwell's equations for lamellar gratings," *J. Opt. Soc. Am. A* 12, 1043-1056 (1995).
16. G. Granet, J. P. Plumey, and J. Chandezon, "Scattering by a periodically corrugated dielectric layer with non-identical faces," *Pure Appl. Opt.* 4, 1-5 (1995).
17. L. Li, G. Granet, J. P. Plumey, and J. Chandezon, "Some topics in extending the C method to coated gratings with different profiles," *Pure Appl. Opt.* 5, 141-156 (1996).
18. The statement "matrix A is of order $O(1)$ " means that every element of A is of order $O(1)$. In the context of this paper saying that a matrix is of order $O(1)$ means that it contains no exponentially growing functions with respect to layer thickness and matrix truncation order.
19. A. K. Cousins and S. C. Gottschalk, "Application of the impedance formalism to diffraction gratings with multiple coating layers," *Appl. Opt.* 29, 4268-4271 (1990).
20. R. Redheffer, "Difference equations and functional equations in transmission-line theory," in *Modern Mathematics for the Engineer*, E. F. Beckenbach, ed. (McGraw-Hill, New York, 1961), Chap. 12, pp. 282-337.
21. G. H. Golub and C. F. Van Loan, *Matrix Computations* (Johns Hopkins University Press, Baltimore, 1983), Chap. 3, p. 30, and Chap. 4, p. 52.